HHS Public Access

Author manuscript

Biosens Bioelectron. Author manuscript; available in PMC 2023 June 23.

Published in final edited form as:

Biosens Bioelectron. 2023 February 15; 222: 114986. doi:10.1016/j.bios.2022.114986.

A novel biosensor for ultrasensitive detection of fungal genes

Muhit Rana[a], **Tugba Yilmaz**[a], **Shirli Cohen**[b], **Sinem Beyhan**[b,c], **Avni A. Argun**[a,*]

[a]Giner, Inc, 89 Rumford Avenue, Newton, MA 02466, United States.

[b]J. Craig Venter Institute (JCVI), 4120 Capricorn Lane La Jolla, CA 92037, United States.

[c]The University of California, San Diego (UCSD), 9500 Gilman Drive # La Jolla CA 92093, United States.

Abstract

Fungal infections are a rapidly increasing public health problem due to their high morbidity and mortality rates, especially in populations with compromised immune systems. Rapid and accurate diagnosis of these diseases is, therefore, necessary to improve the prognosis of afflicted patients. Unfortunately, current clinical chemistry practice relies on lengthy culturing methods that are insufficient to meet the fast turnaround requirements. Here we present a cost-effective and robust nucleic acid sensor that can identify the presence of histoplasmosis causing fungal genes, in whole blood or Bronchoalveolar lavage (BAL) samples, far earlier than current methods. Our novel assay involves the hybridization of target gene sequences with immobilized nucleic acid probes, allowing direct, label-free detection of *Hcp100*, *CBP1*, and M antigen genes through electrochemical analysis. The resultant current is attributed to the presence of fungal targets in the sample solution. The assay provides ultra-sensitive detection of DNA molecules with a limit of detection (LOD) values down to 100 aM, sufficient to meet the clinical diagnostic need. In addition, the turnaround time for the sample to result is less than 90 minutes compared to the current clinical procedure's turnaround time of 3–4 weeks.

Keywords

histoplasmosis; fungal; gene; electrochemical; DNA; detection

1. Introduction

Histoplasma capsulatum is a dimorphic fungus (Simon et al. 2010), which can cause a life-threatening pulmonary infection called histoplasmosis (Brown et al. 2012),(Bahr et al. 2015). *Histoplasma capsulatum* is found as a hyaline mold at room temperature (Beyhan et al. 2013), which is converted to yeast cells that cause pneumonia when inhaled (Azar and

*Correspondence: aargun@ginerinc.com.

Author Contributions

A.A and M.R conceived the study and M.R. designed the experiments. M.R, T.Y., S.C. and S.B. performed the bioinformatics, identified, down selected, and designed the oligos. M.R performed the absence test, sensitivity, specificity, and detection experiments in whole blood, and BAL samples. T.Y helped with absence tests, sensitivity, and selectivity studies in buffer and whole blood samples (for *Hcp100* gene detection). S.C. and S.B. have provided spiked blood and BAL samples and *H. capsulatum* gDNA and contributed intellectually to the scientific discussion. M.R, T.Y and A.A wrote the manuscript.

Hage 2017a). *Histoplasma* species can be found throughout the world; however, they are endemic to Africa, Central America, and North America. In the United States, they are the most common cause of fungal respiratory infections. (Bahr et al. 2015; Kasuga, Taylor, and White 1999; Kasuga et al. 2003).

Immunocompromised patients with elevated risk factors such as bone marrow and organ transplantation, AIDS, leukemia, hematologic malignancy, and chemotherapy (Brown et al. 2012) are at 10–15 times higher risk of getting infected with *Histoplasma* (Drak Alsibai et al. 2020). People with poor immune systems who are in contact with soils daily, such as farmers and construction workers, have the most significant risk of infection. After inhaling the spores, symptoms usually develop within one to three weeks, but a diagnosis is not usually determined until six months later. Around 50% of the people infected with the spores are asymptomatic, and 5–10% of cases become severe with long-term lung problems (Thompson 2011). Therefore, rapid, and early diagnosis of histoplasmosis is vital.

Accurate diagnosis has never been straightforward for endemic mycoses (Kozel and Wickes 2014). Despite the prevalence of fungal infections and their threat to human health, there is no point of care (POC) clinical device available for early diagnosis. Current available diagnoses, which may take several weeks, often do not provide a definitive diagnosis, and sensitivity and specificity are usually low (Kauffman 2007; Saubolle, McKellar, and Sussland 2007). Chest CT scans, biopsy, culture, and microscopy of stained tissue samples can assist with diagnosis, but sampling is highly invasive, and turnaround times can be weeks to months (Azar and Hage 2017b). Therefore, our sensor platform has the clinical potential to provide clinicians with a tool for accurately diagnosing fungal infections. In addition, this preclinical tool can be further investigated, validated with a large sample cohort, and well justified with immediate utilization in clinical and primary care settings for routine health monitoring to lessen the severity of fungal infections.

The typical diagnostic for fungal infection includes culturing clinical specimens on a suitable media such as Sabouraud media (Guimaraes, Nosanchuk, and Zancope-Oliveira 2006) followed by a demonstration of the microorganism presence using direct microscopy on stained clinical samples. However, this method requires a prolonged time and experienced personnel to perform (Simon et al. 2010). Other methods include antigen detection(Alvarado et al. 2020), serology, histopathology, and cytopathology (Azar and Hage 2017a). Molecular detection methods, like PCR, offer higher sensitivity and shorter turnaround times but they require intense sample purification, often yield false positives due to the amplification of non-targets (Kami et al. 2001) and it is challenging to adapt these complex techniques for point of care applications. Another technique, fluorescence *in situ* hybridization (FISH), utilizes fluorescent probes for the detection of DNA sequences; however, it requires labeling steps and offers low sensitivity. (Levsky and Singer 2003). Finally, Ostrov and coworkers developed a modular yeast biosensor for POC applications; however, their biosensors did not show differential detection for *H. capsulatum* since the developed sensor also detected *Paracoccidioides brasiliensis* strains (Ostrov et al. 2017). In summary, none of these methods have the required diagnostic sensitivity and clinical utility to detect *Histoplasma* in relevant biological samples (Azar and Hage 2017a).

DNA hybridization is a significant biological event used in biosensors as it allows the detection of specific DNA regions (Rana et al. 2016; Yilmaz and Goluch 2021). DNA probes can be designed as a recognition element to detect single-stranded target DNA molecules (Tichoniuk et al. 2010). Electrochemical DNA biosensors offer high sensitivity, fast response times, portability, and low cost, making them attractive for point-of-care applications (Ronkainen, Halsall, and Heineman 2010; Wang 2000). (Lei, Chen, and Mulchandani 2006) Herein, we report an enzymatic DNA-based electrochemical assay to accurately measure targeted fungal gene sequences in whole blood, and bronchoalveolar lavage (BAL) samples. The innovation of the assay is to utilize 96-well plates functionalized with nucleic acid probes for capturing target genes of *H. capsulatum* via DNA hybridization and to quantify the abundance of target fungi by electrochemical detection. Using specific DNA hybridization probes, our assay detects predetermined gene sequence biomarkers obtained from prior clinical studies (Martagon-Villamil et al. 2003; Simon et al. 2010) as well as new identified disease biomarkers validated in this study.

To the best of our knowledge, currently, no point of care (POC) test is available for the diagnosis of histoplasmosis. Therefore, it is imperative to provide clinicians with a reliable tool for accurate diagnosis that can rapidly identify the presence of these endemic fungi in patient samples. This is the first report to date on the early detection of *Histoplasma*-specific fungal genes.

2. Materials and Methods

2.1. Materials and Equipment

All oligonucleotide (the custom capture probes, label probes as P1, P2, and P3, and targets for *Hcp100*, M antigen, and *CBP1* gene regions of *H. capsulatum*) sequences were purchased from Integrated DNA Technologies (IDT), USA, and their sequence information is mentioned in the supplementary information (Table S1–S3). Streptavidin Poly-HRP80 conjugate (Catalog # 65R-S120) was purchased from Fitzgerald Industries International, Acton, MA. Streptavidin-coated 96 well plates and Blocker BSA (10%) in PBS (Catalog # 37525) were purchased from Thermo Scientific. 3,3’,5,5’-tetramethylbenzidine (TMB) substrate solution was bought from Surmodics IVD Inc, Eden Prairie, MN 55344. 20 X PBS-T buffer was from Thermo Fisher, while 10 X PBS buffer (pH 7.4), TE buffer (pH 8.0), and DEPC-treated water was procured from Invitrogen. Biotin (Catalog # B4501), H_2SO_4 and $MgCl_2$, and all other reagents were purchased from Sigma-Aldrich, St. Louis, MO 63103, USA. Invitrogen’s Ultrapure DNase-free, RNase-free DEPC treated water (catalog # 4387937) was used in all studies. All commercial blood, and BAL (de-identified pooled) fluids were purchased from BioIVT, Westbury, NY, and tested at Giner’s BSL-2 lab facility. Screen-printed carbon electrodes (Metrohm Dropsens DRP-110) were purchased from Metrohm USA Inc., Riverview, FL. The USB-powered potentiostat (Model number: EmStat3+, Potential range ±3 V or ±4 V, and Current ranges 1 nA to 10 mA or 100 mA) was obtained from PalmSens BV, Houten, Netherlands.

2.2. Methods

2.2.1. Experimental stock preparation—Purchased DNA oligonucleotides were resuspended in TE buffer and stored at −20°C as DNA stocks. DNA probe immobilization and target hybridization buffers were prepared with 1X PBS buffer, including 20 mM $MgCl_2$. In addition, 1X Phosphate Buffered Saline-Tween (PBS-T) buffer and 1X PBS buffer were prepared as washing solutions from the buffer stock solutions. The poly-HRP80-Streptavidin conjugate was diluted in 1X PBS buffer, including 1% BSA at required dilution rates. In addition, 40 μM of freshly prepared biotin solution was prepared in nuclease free DEPC treated water. H_2SO_4 stock solution was diluted with DI water to obtain 0.5 M H_2SO_4 solution. DEPC-treated water was used for all other solutions preparation throughout the experiments.

2.2.2. Assay Development—Herein, we developed an enzymatic sensing system to detect fungal genomic DNA utilizing a single-stranded capture probe (Cp) and three labeling oligonucleotide probes (P1, P2, and P3), as shown in Figure 1. Briefly, the capture probe was designed to hybridize with a nucleic acid region on single-stranded target DNA. This probe was modified with biotin at its 5’ end to attach to the streptavidin-coated 96-well plate surface. After the 25 nM of capture probe was immobilized on the plate surface, the sample solution containing single-stranded target DNA molecules was added to the system. This study designed synthetic target DNA molecules as 133 bps long for *Hcp100*, 181 bps for *CBP1*, and 93 bps oligos for M antigen.

After hybridization, the wells were washed three times with 1X PBS-T buffer and each well was treated with 40 μM of freshly prepared biotin solution for 10 min at room temperature (RT) to avoid possible non-specific bindings.100 uL of the labeling probe mixture, which was previously prepared in one tube to be 25 nM of each P1, P2, and P3 probe, was added to the wells to hybridize along the length of the target DNA. After washing the wells with buffer solution, 30X Streptavidin PolyHRP80 conjugate (prepared with 10X of 10% Blocker BSA solution with PBS) was introduced to the wells to attach to the labeling probes by biotin-streptavidin interaction. After the washing step, 100 μL of stock TMB was added to the wells. Poly-HRP catalyzes the oxidation of TMB in the presence of hydrogen peroxide. After 10 minutes 50 μL of 0.5M H_2SO_4 was added to the system to stop the reaction. Each well was analyzed by UV/Vis spectroscopy (at 450 nm) and chronoamperometry. The oxidized form of TMB can be measured by chronoamperometry once converted to the diimine form in acidic conditions.

2.2.3. Sensitivity measurements—Spectrophotometric and electrochemical measurements were performed using various concentrations of target DNAs designed separately for the M antigen, *Hcp100*, and *CBP1* gene regions. Ranging concentrations of target DNA (10 nM down to 100 aM for the M antigen, and *CBP1* genes; 1 nM down to 61 fM for the *Hcp100* gene) were added to the wells to hybridize with the 25 nM of accordingly designed capture probes. Control experiments were performed in the absence of the target gene while keeping every other parameter unchanged. For all electrochemical measurements in this research, 70 uL of TMB solution was added onto the electrode surface, followed by amperometric measurements. An operating potential of 125 mV was applied to decay

the transient currents to a steady-state value. The time required for this was determined as 30 seconds in this study. Sharply increasing current implies that TMB reduction has been achieved.

2.2.4. Specificity measurements—The assay's specificity was evaluated for each target sequence. A complex cocktail mixture of non-target genes was prepared to show that the assay can detect only the targeted gene sequence *in vitro* PBS buffer as well as in exogenously enriched commercial human whole blood and BAL samples.

2.2.5. Detection in Blood, and BAL Samples—The unprocessed (no anticoagulant/ filtration, storage condition at −20° C or colder) human whole blood, and BAL samples were utilized to demonstrate the assay preclinical utility. Prior to testing, 5 μL of blood, and/or BAL samples were diluted with 95 μL of reaction buffer to the final volume of 100 μL (20X dilution). The specimens (Blood, and BAL samples) were spiked with 1 nM of the target gene, *CBP1. Hcp100* and M antigen both genes were tested in exogenously enriched commercial human whole blood. Both exogenously enriched (spiked) and unspiked samples were tested, followed by the remaining enzymatic steps as described above.

3. Results and Discussion

Our designed assay uses biotinylated DNA capture probes functionalized on a surface (such as a streptavidin-coated 96-well plate surface) to capture target DNA sequences precisely. Upon capture, the target DNA is tagged with additional sequence-specific label probes (P1, P2, and P3). An enzyme such as poly-HRP is then attached to these label probes, which catalyzes the oxidation of 3,3′,5,5′-Tetramethylbenzidine (TMB) in the presence of hydrogen peroxide, and the oxidized form of TMB is reduced by chronoamperometry once converted to the diimine form in acidic conditions (Figures 1 and S1).

Since the HRP enzyme oxidizes the TMB molecule, the subsequent chronoamperometric analysis focuses on the cathodic current produced when the TMB is reduced. Current peaks observed during this reduction step are proportional to the amount of TMB in solution and thus the targeted DNA.

3.1. Development and optimization of the assay with the *Hcp100* gene

DNA hybridization between designed capture probes and target DNA was confirmed before assay development. The temperature-mediated DNA hybridization efficiency was characterized using multiple methods, including UV-Vis spectroscopy and fluorogenic assay, before testing with our electrochemical assay (See Figure S2–S3). We have used a set of specific probes designed for this study; a complete list of sequences is provided as Tables S1–S3 in Supporting information.

3.1.1. Assay Optimization: Background determination in PBS—To optimize our assay development and electrochemical detection, we selected and started with the *Hcp100* gene, one of the selected gene panels for this study. As shown in Figure 2A, wells with target DNA show a significant difference in absorbance as compared to the control wells that only contain the capture probe (Cp), or Cp and target (T), or Cp and amplification

probes, Ap (no target DNA). Figure 2A (right) shows that signals obtained from absorbance measurement or optical density (OD) of TMB are strong enough to distinguish from the background signal and that the signal from the amperometry (data not shown) matches up well with the absorbance signal from the TMB for 200 pM of *Hcp100* gene target.

3.1.2. Sensitivity testing of *Hcp100* genes in PBS.—As shown in Figure 2B–C, we observed a significant amount of signal enhancement in the presence of various target concentrations (1 nM down to 25 pM) as compared to the control experiment. We validated this signal enhancement through colorimetric and UV-Vis measurement at 450 nm (Figure 2B), and the spectroscopic 3-sigma rule based LOD is at the pM level. The limit of detection (LOD) is calculated, followed by the 3-sigma rule. The equation is, LOD=3.3 x standard deviation of the regression line (σ) /Slope(S). A 3σ-rule is widely used to determine the signal-to-noise ratio for estimating the detection limit. (Rana et al. 2016; Kumar et al. 2022; Novick, Zhao, and Yang 2017; Kim et al. 2019; Desai et al. 2018; Cipra et al. 1990) The sensitivity testing confirmed the LOD is within pM ranges and showed that the sensitivity (Figure 2B, R^2=0.9879) is highly reproducible.

We also observed a similar finding from the electrochemical analysis. Additionally, in order to normalize the intra-assay or plate-to-plate variances, we normalized the data with background subtraction. Overall, the standard curve with R^2=0.9811 value from electrochemical amperometric peak analysis (Figure 2C) shows excellent linearity and correlation between peak current and concentration of target DNA.

3.2. Assay Versatility: *In vitro* absence test of *CBP1* and M antigen genes.

As shown in Figure 3, wells with target DNA show a significant difference in optical density (OD) as compared to the control wells that only contain the capture probe (Cp), or Cp and target (T), or Cp and amplification probes, Ap (no target DNA), or Cp + Ap + T. Figure 3A show that signals obtained from absorbance measurement of TMB are strong enough (Cp+Ap+T) to distinguish from the background signal (Cp or Cp+T or Cp+Ap) and that the signal from the amperometry (data not shown) matches up well with the absorbance signal from the TMB for 1 nM of *CBP1* or M antigen gene target.

Additionally, in order to normalize the intra-assay or plate-to-plate variances, in Figure 3B–C we normalized the data with background subtraction and represented it as absorbance (%) for *CBP1* (green color) and M antigen (orange color) gene. This result re-confirms that the assay's absence test is reproducible, and the functionality of the assay is promising to evaluate the sensitivity and specificity of *CBP1* and M antigen genes in biological samples.

3.3. Sensitivity Validation: Sensitivity Evaluation of *CBP1* and M antigen in Blood Samples.

As shown in Figure 4 (A–D), we observed a significant amount of signal enhancement in various target concentrations (10 nM down to 100 aM) settings compared to the control experiment for *CBP1* and M antigen genes (highly reported genes for *Histoplasma* compared to the other gene panels) in the human whole blood samples. Furthermore, we validated this signal enhancement through UV-Vis measurement at 450 nm with a statistical LOD of 3.84

fM for *CBP1* (Figure 4A, R^2=0.997) and a femtomolar (fM) level of electrochemical LOD for *CBP1* (Figure 4B, R^2=0.9966) in human whole blood samples. A representative series of electrochemical chronoamperometry measurement of *CBP-1* is shown in Figure S4. The log scale-based low and high ranges of concentrations and their data analysis and LOD are shown in Figure S5, R^2=0.9696).

3.4. Specificity Validation: Specificity Evaluation of *CBP1* and M antigen in Blood Samples.

To verify our assay specificity, we utilized whole blood samples to detect exogenously enriched *CBP1* (Figure 5 A–B) and M antigen (Figure 5 C–D) gene targets. As seen in Figure 5, the assay successfully detected 1 nM of *CBP1* and M antigen in complex biological matrices. Next, we tested the specificity of *CBP1* and M antigen genes in clinical blood samples (Figures 5 A–D). In the absence of target (Figure 5 A–B and C–D) the "sandwich" assay showed a very light blue color (background) that transitioned to light to dark yellow color in the presence of H_2SO_4. When the target was present, a bright and dark blue color was observed due to poly-HRP triggered oxidation of TMB, which transitioned to orange when acid was added (Figure 5A, inset).

After the initial confirmation of spectroscopic and electrochemical sensitivity of *CBP1* gene, we repeated the spectroscopic (Figure 4C) and electrochemical (Figure 4D) sensitivity for M antigen gene in human whole blood samples. Again, we observed highly reproducible dynamic ranges of sensitivity. Overall, the standard curve with R^2=0.9966 value from electrochemical amperometry peak analysis (Figure 4B, inset) shows excellent linearity and correlation between peak current and concentration of target DNA.

Overall, UV-Vis and electrochemical signals from human whole blood samples shown in Figure 5 indicate that the assay is highly specific and produces less than 2% signal with non-specific target analytes. Similarly, we tested the specificity of our enzyme-linked assay for sensitive detection of the *Hcp100* gene target from a complex cocktail mixture of the non-target gene in whole blood samples (Figure S8).

3.5. Preclinical utility validation: Testing of complex BAL sample.

To verify assay versatility and preclinical utility, we tested our platform with commercial Bronchoalveolar Lavage (BAL) samples. As seen in Figure 6, the assay successfully detected 1 nM of the *CBP1* gene in a spiked BAL sample. When the target was present a vivid blue color was observed. Overall, UV-Vis, colorimetric images (Figure 6, inset) and electrochemical signals from human BAL sample (from commercial source-BioIVT) indicate that the assay is highly specific and able to detect the correct target in PBS, Blood (previously shown in Figure 2–5), and BAL samples. This data (Figure 6) confirms assay versatility and preclinical utility in different challenging biological samples. We also validated of our sensor with a randomized unbiased sample where the target genes were exogenously enriched in individual biological matrixes and then extracted prior to testing (Figure S9).

4. Conclusion and Outlook

Fungal infections are increasingly crucial for human health. Late diagnosis can be life-threatening and compromise the effectiveness of available therapeutic interventions. Accurate and early diagnosis can be a lifesaver to assist in developing therapeutic agents, directing antifungal management, and preventing misuse of antibiotics. In this work, we have investigated how a practical DNA-based electrochemical sensor can precisely detect single target gene using sequence-specific biotinylated probes and the streptavidin poly-HRP80 conjugates. We have demonstrated that strategic involvement of poly-HRP80 conjugates enzyme within the probe-target hybridization provided highly sensitive detection of DNA levels (as low as 100 aM) in blood and BAL samples. This study demonstrates that the challenges of accurate diagnosis of fungal genes can be addressed using a biosensor assay that involves integration of poly-HRP80 conjugates enzyme and sequence-specific capture probe (Cp) and amplification probes (P1, P2, and P3) followed by the TMB-H_2O_2 reaction. In addition, the preclinical utility of this DNA sensor platform is not restricted to detect only fungal genes. The versatility of this technology allows for target-specific probe design to detect other pathogen genes and high throughput performance is enabled by the use of standard streptavidin 96-well plates. Using the same platform, future work will include detection of other clinically relevant infectious genes and disease biomarkers with different probes. Furthermore, we envision to develop a practical POC test for rapid and accurate detection of *Histoplasma* genomic sequences in blood (for systemic infections), sputum, and bronchoalveolar lavage fluid (BAL, for respiratory infections) to address unmet diagnostics need for histoplasmosis.

Supplementary Material

Refer to Web version on PubMed Central for supplementary material.

Acknowledgements

M.R, T.Y, S.C, S.B, and A.A acknowledge the funding support from National Institutes of Health (NIH), Department of Health and Human Services (DHHS), National Institute of Allergy, and Infectious Diseases (NIAID) through SBIR Phase I Contract (Contract # 75N930020C00034). Additionally, S.B. is supported by the NIAID (Grant # R01AI137418). We acknowledge Mr. Andrew Weber's contribution to proofread the manuscript.

References

Alvarado P, Perez-Rojas Y, Zambrano EA, Gonzatti MI, and Roschman-Gonzalez A. 2020. J Microbiol Methods, 175: 105981. [PubMed: 32534998]

Azar MM, and Hage CA. 2017a. J Clin Microbiol, 55: 1612–20. [PubMed: 28275076]

Azar Marwan M., and Hage Chadi A.. 2017b. Journal of Clinical Microbiology, 55: 1612. [PubMed: 28275076]

Bahr NC, Antinori S, Wheat LJ, and Sarosi GA. 2015. Curr Trop Med Rep, 2: 70–80. [PubMed: 26279969]

Beyhan S, Gutierrez M, Voorhies M, and Sil A. 2013. PLoS Biol, 11: e1001614. [PubMed: 23935449]

Brown GD, Denning DW, Gow NA, Levitz SM, Netea MG, and White TC. 2012. Sci Transl Med, 4: 165rv13.

Cipra T, Fuchs A, Formanek J, Kubat J, Mikiskova H, Zajicek P, and Dvorak J. 1990. Act Nerv Super (Praha), 32: 283–91. [PubMed: 2082646]

Desai D, Kumar A, Bose D, and Datta M. 2018. Biosens Bioelectron, 105: 90–94. [PubMed: 29412950]

Drak Alsibai K, Couppie P, Blanchet D, Adenis A, Epelboin L, Blaizot R, Louvel D, Djossou F, Demar M, and Nacher M. 2020. Front Cell Infect Microbiol, 10: 591974. [PubMed: 33194840]

Guimaraes AJ, Nosanchuk JD, and Zancope-Oliveira RM. 2006. Braz J Microbiol, 37: 1–13. [PubMed: 20445761]

Kami M, Fukui T, Ogawa S, Kazuyama Y, Machida U, Tanaka Y, Kanda Y, Kashima T, Yamazaki Y, Hamaki T, Mori S, Akiyama H, Mutou Y, Sakamaki H, Osumi K, Kimura S, and Hirai H. 2001. Clin Infect Dis, 33: 1504–12. [PubMed: 11588697]

Kasuga T, Taylor JW, and White TJ. 1999. J Clin Microbiol, 37: 653–63. [PubMed: 9986828]

Kasuga T, White TJ, Koenig G, McEwen J, Restrepo A, Castaneda E, Da Silva Lacaz C, Heins-Vaccari EM, De Freitas RS, Zancope-Oliveira RM, Qin Z, Negroni R, Carter DA, Mikami Y, Tamura M, Taylor ML, Miller GF, Poonwan N, and Taylor JW. 2003. Mol Ecol, 12: 3383–401. [PubMed: 14629354]

Kauffman CA 2007. Clin Microbiol Rev, 20: 115–32. [PubMed: 17223625]

Kim JH, Cho CH, Ryu MY, Kim JG, Lee SJ, Park TJ, and Park JP. 2019. PLoS One, 14: e0222144. [PubMed: 31553730]

Kozel TR, and Wickes B. 2014. Cold Spring Harb Perspect Med, 4: a019299. [PubMed: 24692193]

Kumar Narendra, Rana Muhit, Geiwitz Michael, Khan Niazul Islam, Catalano Matthew, Ortiz-Marquez Juan C., Kitadai Hikari, Weber Andrew, Dweik Badawi, Ling Xi, van Opijnen Tim, Argun Avni A., and Burch Kenneth S.. 2022. ACS Nano, 16: 3704–14. [PubMed: 35201755]

Lei Y, Chen W, and Mulchandani A. 2006. Anal Chim Acta, 568: 200–10. [PubMed: 17761261]

Levsky JM, and Singer RH. 2003. J Cell Sci, 116: 2833–8. [PubMed: 12808017]

Martagon-Villamil J, Shrestha N, Sholtis M, Isada CM, Hall GS, Bryne T, Lodge BA, Reller LB, and Procop GW. 2003. J Clin Microbiol, 41: 1295–8. [PubMed: 12624071]

Novick SJ, Zhao W, and Yang H. 2017. PDA J Pharm Sci Technol, 71: 20–32. [PubMed: 27516490]

Ostrov N, Jimenez M, Billerbeck S, Brisbois J, Matragrano J, Ager A, and Cornish VW. 2017. Sci Adv, 3: e1603221. [PubMed: 28782007]

Rana Muhit, Balcioglu Mustafa, Kovach Maya, Mustafa Salih Hizir Neil M. Robertson, Khan Irfan, and Yigit Mehmet V.. 2016. Chemical Communications, 52: 3524–27. [PubMed: 26839925]

Ronkainen NJ, Halsall HB, and Heineman WR. 2010. Chem Soc Rev, 39: 1747–63. [PubMed: 20419217]

Saubolle MA, McKellar PP, and Sussland D. 2007. J Clin Microbiol, 45: 26–30. [PubMed: 17108067]

Simon S, Veron V, Boukhari R, Blanchet D, and Aznar C. 2010. Diagn Microbiol Infect Dis, 66: 268–73. [PubMed: 20159374]

Song L, Shan D, Zhao M, Pink BA, Minnehan KA, York L, Gardel M, Sullivan S, Phillips AF, Hayman RB, Walt DR, and Duffy DC. 2013. Anal Chem, 85: 1932–9. [PubMed: 23331316]

Thompson GR 3rd. 2011. Semin Respir Crit Care Med, 32: 754–63. [PubMed: 22167403]

Tichoniuk M, Gwiazdowska D, Ligaj M, and Filipiak M. 2010. Biosens Bioelectron, 26: 1618–23. [PubMed: 20829023]

Wang J 2000. Nucleic Acids Res, 28: 3011–6. [PubMed: 10931914]

Yilmaz Tugba, and Goluch Edgar D.. 2021. TrAC Trends in Analytical Chemistry, 144: 116416.

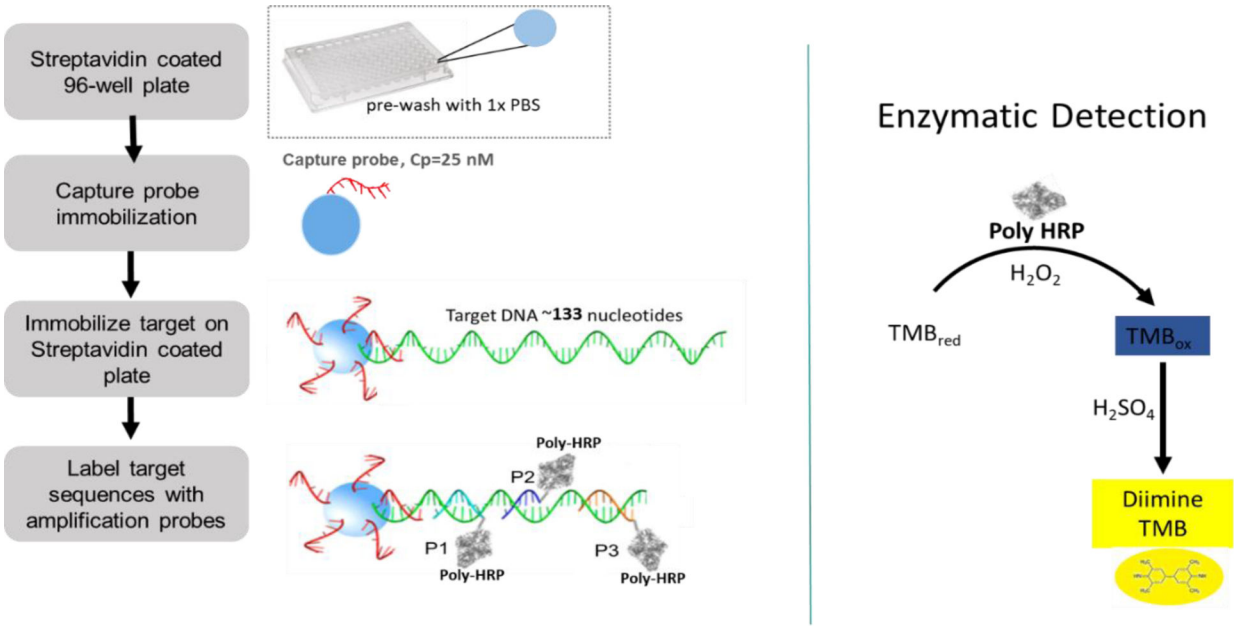

Figure 1:

Principle of our electrochemical DNA sensor and the flow scheme for hybridization and detection of Histoplasma-specific oligonucleotides. Functionalization of streptavidin-coated 96 well plate with capture probe and the operation of our assay that monitors enzymatically amplified electrochemical signal. Figure adapted from Song et al. 2013.(Song et al. 2013)

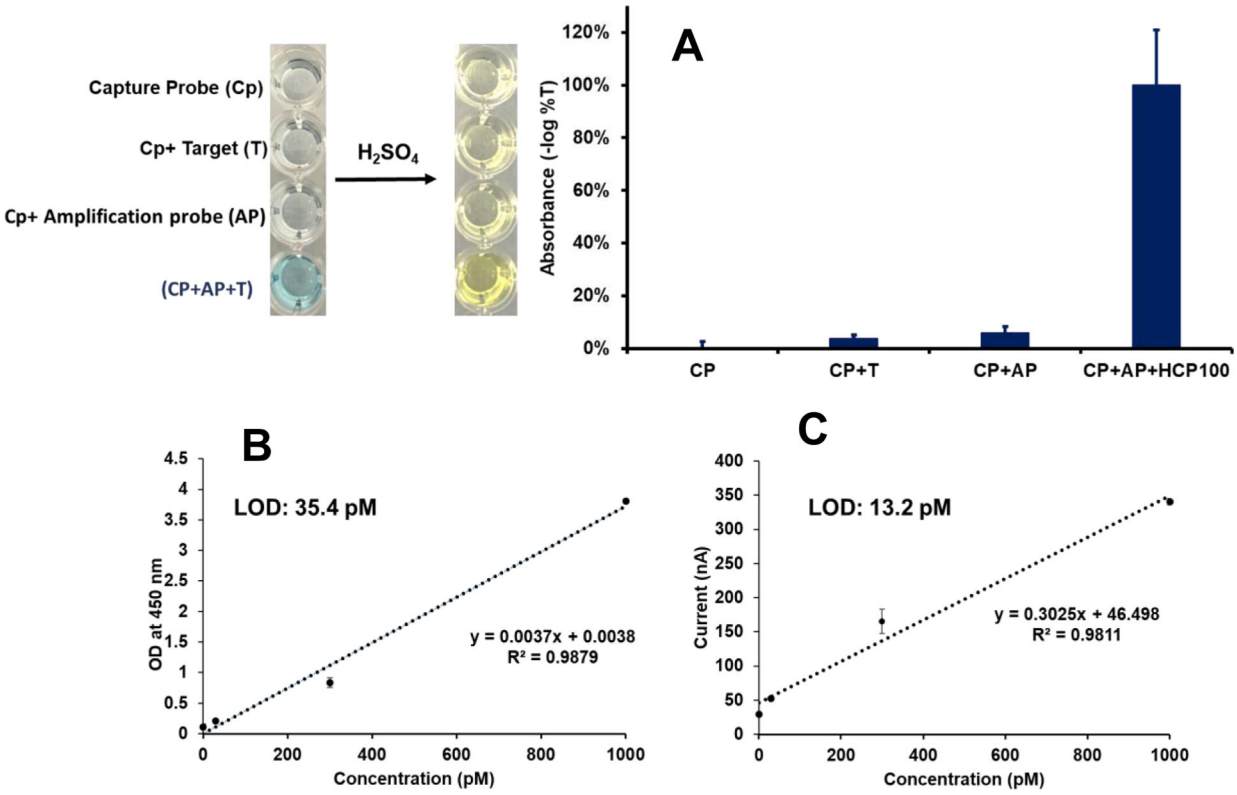

Figure 2.

A. Absence test and assay performance evaluation of our assay in PBS buffer. Relative signal of the enzyme-linked assay with no DNA target (control) and 1 nM concentration of *Hcp100* DNA target. Results from images and absorbance reading (%). All experiments were performed in triplicate (n=3). **B-C.** Sensitivity testing. B. Spectroscopic LOD=35.4 pM and C. Electrochemical sensitivity, LOD=13.2 pM (n=3). All experiments were performed in triplicate (n=3).

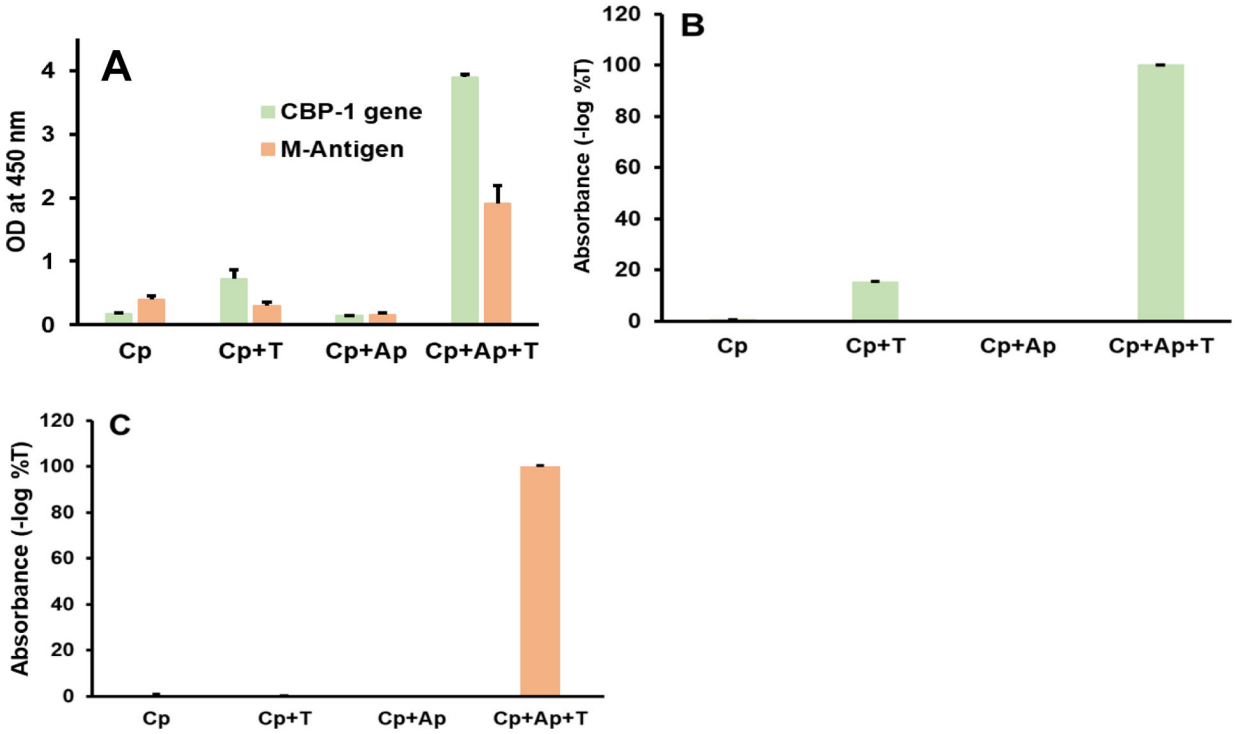

Figure 3.

Absence test and assay performance evaluation in buffer. Relative signal of the enzyme-linked assay with no DNA target (control) and 1 nM concentration of *CBP1* and M antigen DNA target. **A.** Results from absorbance reading at 450 nm; and **B-C.** after employing statistical background correction absorbance measurement in % from *CBP1* and M antigen gene. All experiments were performed in triplicate (n=3).

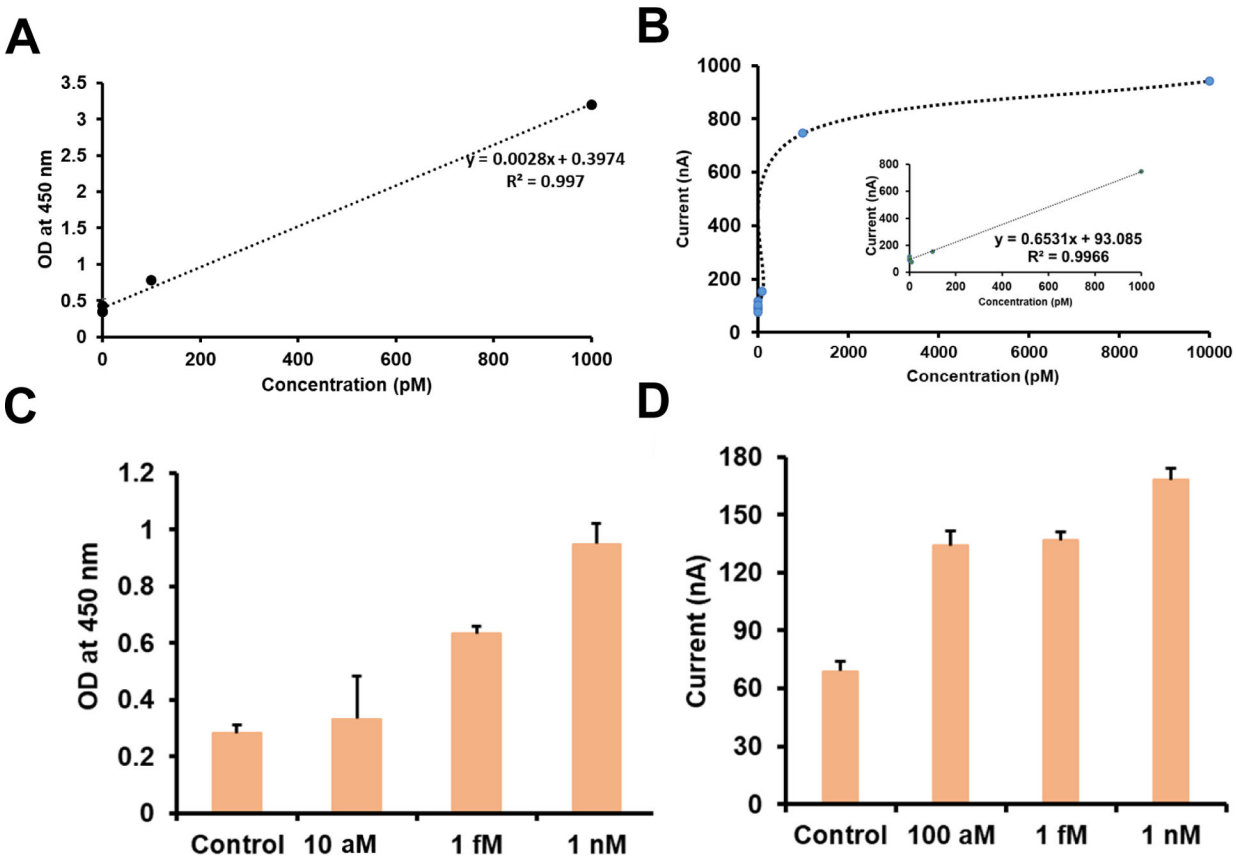

Figure 4.

A-D. Sensitivity testing in human whole blood samples. Dynamic range of of *CBP1* gene; **A**. Spectroscopic LOD=3.84 fM; **B**. Electrochemical LOD= <1 fM (n=3). Inset: R^2=0.9966 from electrochemical amperometry peak analysis. Dynamic range of M antigen gene; **C-D.** Spectroscopic and electrochemical sensitivity, LOD is aM level (n=3).

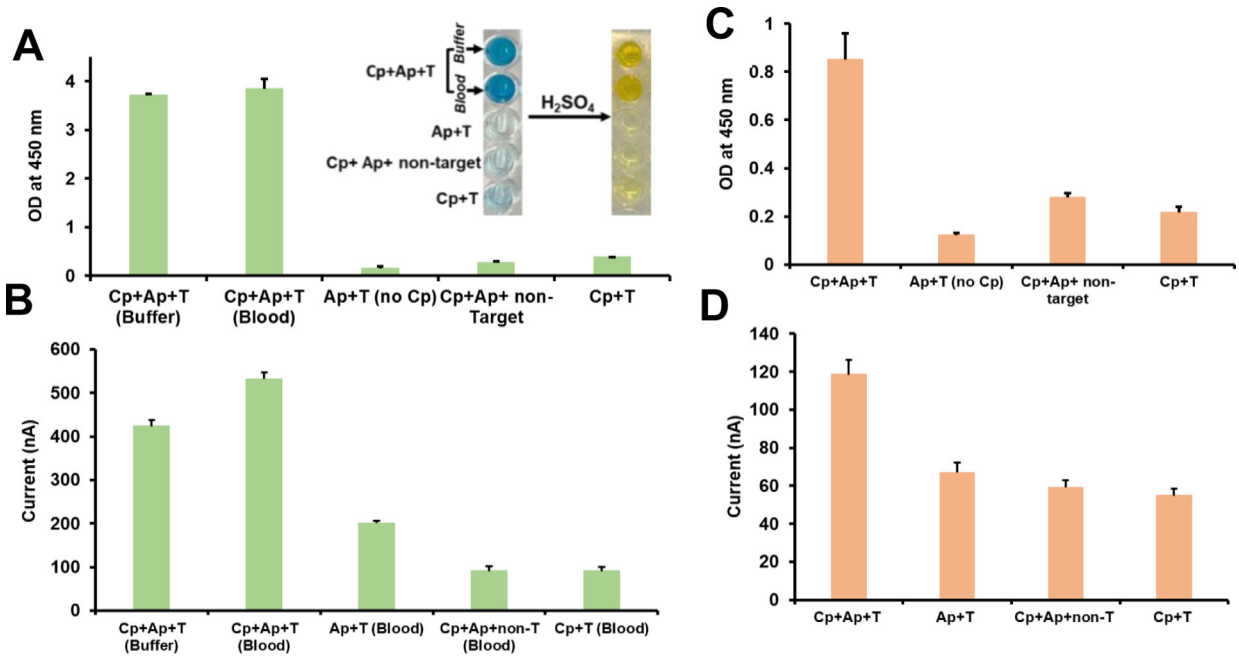

Figure 5.

A-D. Specificity testing of *CBP1* and M antigen genes in whole blood samples. The exogenous *CBP1* and M antigen genes detection in commercial whole blood and compared to buffer samples in presence of non-target. Inset: Images of well plate. Upper Left panel: Absorbance reading; Lower Left panel: Chronoamperometry (n=3). Specificity confirms the *CBP1* and M antigen genes detection in cocktail mixture. (n =3)

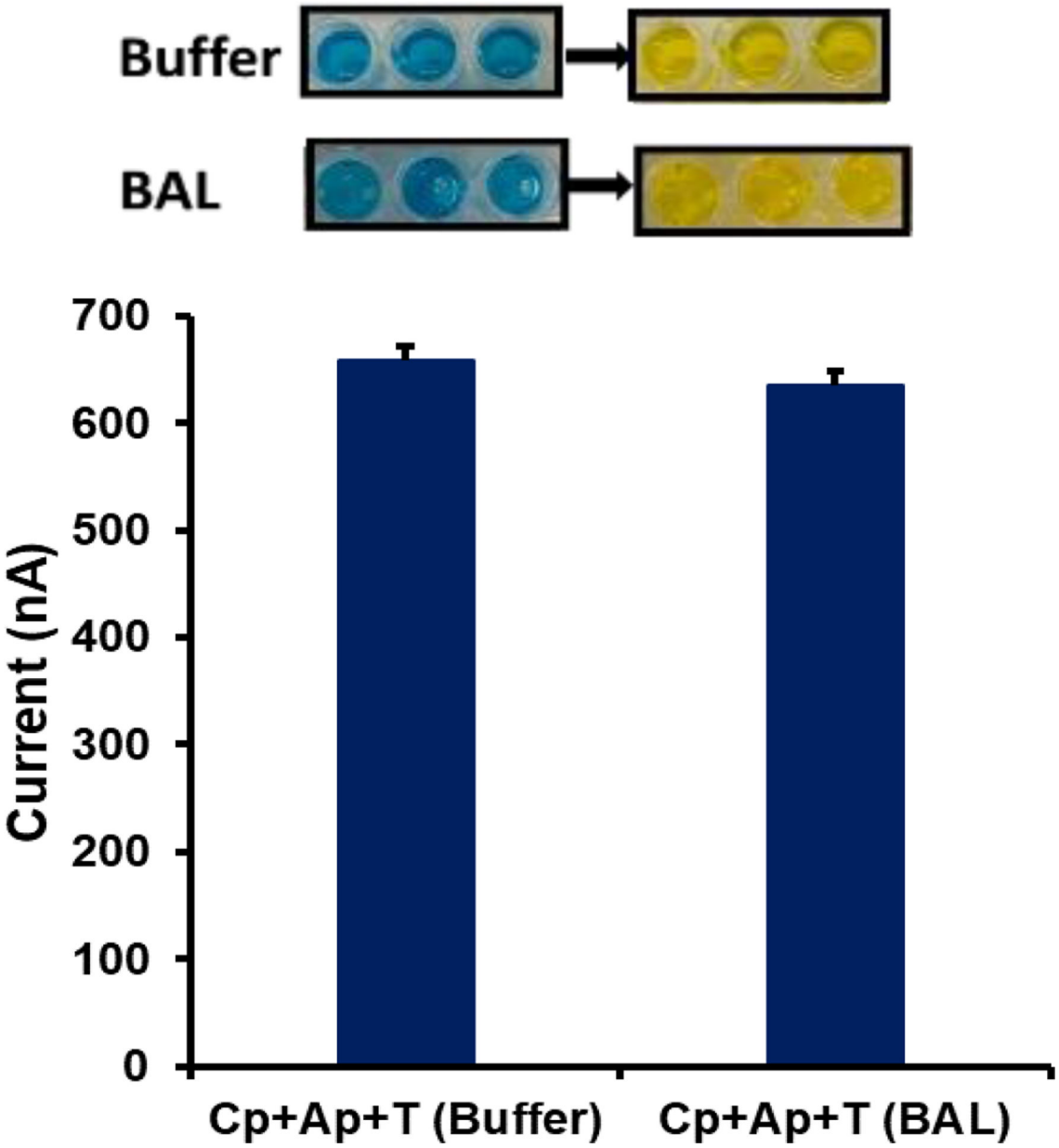

Figure 6.

Preclinical utility validation. Positive control testing of *CBP1* gene in PBS vs BAL samples. Relative signal of the enzyme-linked assay with 1 nM of *CBP1* DNA target in PBS vs BAL samples, to cross-validate the signal variances. Electrochemical measurement confirms the *CBP1* gene detection in BAL samples (n=3).